



A comparative study of irreversible magnetisation and pinning force density in (RE)Ba₂Cu₃O_{7- δ} and some other high- T_c compounds in view of a novel scaling scheme

M. Jirsa^{*}, L. Půst

Institute of Physics, Academy of Sciences of the Czech Republic, Na Slovance 2, CZ-18040 Praha 8, Czech Republic

Received 12 May 1997; revised 26 July 1997; accepted 26 July 1997

Abstract

We examined an extended set of experimental data on scaling of the field dependencies of the critical current density $j_s(B)$ and/or the related pinning force density $F(B)$ as found in literature for various high- T_c single crystals, mainly (RE)Ba₂Cu₃O_{7- δ} (RE \equiv rare earth), exhibiting the fishtail effect. The $j_s(B)$ and/or $F(B)$ curves, normalised with respect to the corresponding (fishtail) maximum, are shown to obey the functional dependencies $j_{sc}(b) = b^m \exp[(m/n)(1 - b^n)]$ and $f(b_f) = b_f^{m+1} \exp\{[(m+1)/m](1 - b_f^n)\}$ where b and b_f are the applied field values normalised with respect to position of the corresponding (fishtail) maximum, and j_{sc} and f are the normalised values of the critical current density, and pinning force density, respectively. A possible link between the presented phenomenological scaling scheme and the theory of collective pinning is discussed. Most of the analyzed data could be well fitted with m set equal to 1 and n left as the only free parameter. n varied from 0.5 to 3.95 but most values fell into the interval (1,2). We point out that the value $n = 3/2$ in the middle of this interval is predicted by the collective pinning theory for the small bundle pinning regime. © 1997 Elsevier Science B.V.

PACS: 74.60 Jg; 74.60 Ge

1. Introduction

The “peak” effect, the still not well understood phenomenon resulting in an enhancement of the critical current density at higher fields and temperatures has in recent years attracted a particular interest. One of the reasons is a potential use in applications, another one is that the “peak” effect can serve as a test probe of our understanding to mecha-

nisms of the vortex pinning in high temperature superconductors. During recent years a large number of papers dealing with different aspects of this phenomenon has been published offering a good platform for generalisation. According to the shape of the magnetisation hysteresis loop (MHL), the high- T_c materials can be divided into two main categories: those with the fishtail shape of the curve (typically (RE)Ba₂Cu₃O_{7- δ} (RE \equiv rare earth, (RE)-123 and similar single crystals) [1–26] and those with the arrow-head shape (Y-124, BiSrCaCuO and other related compounds) [27–40]. It is probably not only an

^{*} Corresponding author. Fax: +420 2 821227; e-mail: jirsa@fzu.cz

accidental coincidence that the former group consists of less anisotropic compounds (with mostly 3D vortex behaviour) while the latter one is formed by highly anisotropic materials where the pancake (2D) vortex regime is usually observed. Except these two main categories, some other specific shapes of the MHL sometimes appear, especially in heavily twinned samples [3,16,23] or in highly oxygen deficient ones [17].

In this paper, we discuss the fishtail effect observed in (RE)-123 samples. The analyzed experimental material collected from literature [1–26] covers a wide variety of sample compositions, preparation processes and experimental techniques.

The fishtail peak is usually attributed to an enhanced pinning due to impurities becoming active at high fields [1–5]. The recent experiments made on single crystals of Y-123 and Tm-123 with an extremely low level of metallic impurities [17–19] showed that the fishtail effect can be reversibly generated and suppressed by varying oxygen content in these samples. High oxygen pressure and a sufficiently high temperature were substantial for the complete suppression of the fishtail effect [18,19] giving evidence that not only the average content but also the homogeneity of the oxygen distribution is important. The same treatment made simultaneously on single crystals prepared from the commonly used yttrium stabilised ZrO₂ crucibles (higher level of impurities) caused only a partial suppression of the fishtail effect. These results convincingly prove that the fishtail maximum is in (RE)-123 single crystals mostly due to pinning on oxygen clusters in inhomogeneously oxygenated samples. Metallic impurities probably activate or at least enhance this process [17–19]. This conclusion has also been supported by annealing experiments made in other laboratories [10] and by effects caused by different metallic dopants added artificially into (RE)-123 compounds [2,5,41].

While the chemical conditions leading to the fishtail behaviour seem to be clear, the understanding of the physical background of this phenomenon is not yet so transparent. We try to look at this problem using a new phenomenological approach.

The fishtail maximum represents a characteristic feature of the MHL that enables normalisation of the curves and investigation of their shape in depen-

dence on temperature. It occurs that in a certain temperature interval the normalised MHLs scale to a single “universal” curve. On basis of the phenomenological scheme developed for (RE)-123 compounds in Refs. [6,7], we derived a simple analytical expression [8] for the universal curve that proved to fit surprisingly well not only our own data but practically all experimental data found in literature. The aim of this paper is to present results of the fit on a wide variety of (RE)-123 samples and to discuss this novel expression with respect to the theory of collective pinning.

2. Model

In Ref. [8] it was shown that the shape of the $j_s(B)$ curve normalised with respect to the coordinates of the fishtail maximum (B_p , j_{sp}) can be in (RE)-123 single crystals well fitted by the expression

$$j_{sc}(b) = b^m \exp\left[\frac{m}{n}(1 - b^n)\right], \quad (1)$$

where $j_{sc} = j_s/j_{sp}$ is the normalised critical current density and $b = B/B_p$ is the normalised magnetic field. The coefficients m and n are consistent with those from Ref. [7] (except that n has an opposite sign) and with the factors κ_E and $(1 - \gamma_E)/[\gamma_E \ln(vB/E)]$, respectively, from Ref. [6]. This type of a functional dependence follows from an interplay of field dependencies of the characteristic current density j_0 and the characteristic activation energy U_0 entering the generally accepted relation [6,42,43]

$$U(T, B, j_s) = U_0(T, B) V\left(\frac{j_s}{j_0(T, B)}\right). \quad (2)$$

Perkins et al. pointed out that scaling of the high-field part of the MHL implies

$$j_0 \propto B^m, U_0 \propto B^{-n}. \quad (3)$$

For the Tm-123 single crystal the authors found that both m and n are close to 1, and V is nearly a logarithmic function. Our analysis made on a large number of different RE-123 single crystals, both measured in our laboratory and found in literature [1–26], has revealed that the scaling properties can be practically always well described by Eq. (1) with m kept equal to 1, and n used as a free parameter.

Schnack et al. [42] developed their general inversion scheme (GIS), intended for determination of the temperature dependencies of j_0 and U_0 , under the assumption that the characteristic quantities are inter-related as

$$U_0(B) \propto [j_0(T, B)]^p, \quad (4)$$

with a parameter p .

Eliminating B from Eq. (3), we find that p in GIS corresponds to $-n/m$ in the present scheme. With m equal to 1, p corresponds to $-n$.

Note that in the model of Perkins et al., the relationship Eq. (4) is not a prediction like in GIS but it is a consequence of the experimentally observed scaling of the irreversible magnetisation. This presents a tool enabling us to deduce type of the pinning regime from the scaling properties of induced currents in the superconductor.

For different pinning regimes, the collective creep theory [43–47] predicts a power-law relation Eq. (4), with discrete values $p = -n/m$ equal to $-3/2$, $-1/2$, 0 , $1/2$, or 1 , according to the particular type of pinning. In the first case, pinning of small bundles, it predicts also the linear preexponential field-dependent term ($m = 1$) and, consequently, $n = 3/2$. In the range of validity of this pinning regime, above the crossover field B_{sb} , the normalised critical current should therefore scale as described by Eq. (1), with $m = 1$ and $n = 3/2$.

However, application of the normalisation conditions

$$j_s(B_p) = j_p, \quad [dj_s(B)/dB]_{B=B_p} = 0 \quad (5)$$

to the corresponding theoretical $j_s(B)$ dependence [45] results in the conclusion that the maximum of the normalised field dependence lies at about $B_p \approx B_{sb}/2$, well below the range of applicability of the given pinning regime. The theory of the small bundle pinning regime describes therefore only the upper, smoothly decreasing part of the curve and does not simply account for the maximum of the fishtail feature.

On the background of the above discussed relations between the microscopic and phenomenological models of creep, the experimentally observed scaling property can be understood as a manifesta-

tion of the well defined pinning regime existing within field and temperature limits of the scaling. It also indicates that a pinning regime similar to the small bundle pinning exists in a much wider field range than predicted by the present microscopic theory.

Scaling properties are often presented in terms of the pinning force density $F = Bj_s$. The alternative relation to Eq. (1) valid for $F(B)$ follows from Eq. (1) and the two necessary conditions of the type Eq. (5), however with j_s replaced by F . Normalising $F(B)$ with respect to its maximum value, $F_p = B_{fp}j_s(B_{fp})$, we need to take into account that position B_{fp} of the maximum on the $F(B)$ curve differs from that of the corresponding $j_s(B)$ curve, B_{jp} . In our scheme, both these values are related as

$$B_{fp} = B_{jp} [(m+1)/m]^{1/n} \quad (6)$$

which follows from the condition $[dF(B)/dB]_{B=B_{fp}} = 0$ in combination with Eq. (1). The second necessary condition, $f(B_{fp}) = F(B_{fp})/F_p = 1$, yields

$$f(b_f) = b_f^{m+1} \exp \left[\frac{m+1}{n} (1 - b_f^n) \right], \quad (7)$$

with $b_f = B/B_{fp}$.

3. Overview and fit of experimental data

In order to check the relations Eqs. (1) and (7), we analyzed a wide range of data published in literature for (RE)-123 and some other compounds. Results of this work are summarised in Tables 1 and 2. The most important characteristics of both the samples and the experimental methods used are attached, more details can be found in the corresponding references. The experimental data (symbols in the present figures) were extracted from the indicated (blown up) figures by taking points equidistantly from the indicated experimental curves. These data were put into the graphical program Origin where, after normalisation, $j_s(B)$ dependencies were fitted with Eq. (1) and $F(B)$ dependencies with Eq. (7). All fits were performed with m set equal to 1 and only n was left as a free parameter. Quality of

Table 1
Comparison of the scaling properties of Y-123 samples

Material	Reference	n	D	Note	Method
YBa ₂ Cu ₃ O _{7-δ} + Au1.2 at %	[3], Fig.1(b)	1.78	j	D208-12, 50 K	SQUID
YBa ₂ Cu ₃ O _{7-δ}	[5], Fig. 5	3.94	j	2515B, plateau, 22–65 K	VSM
YBa ₂ Cu _{2.975} Ni _{0.025} O _{7-δ}	[5], Fig. 7	2.7	j	26292B, plateau, 25–58 K	VSM
YBa ₂ Cu _{2.99} Ni _{0.01} O _{7-δ}	[5], Fig. 6	0.8–1.7	j	2724A, 30–58 K	VSM
YBa ₂ Cu ₃ O _{7-δ}	[9], Fig. 2	0.63	f	No. 6, unirr., 40–80 K	SQUID
YBa ₂ Cu ₃ O _{6.79}	[10], Fig.5(b)	1.6	j	No. 13, 60 K	SQUID
YBa ₂ Cu ₃ O _{7-δ}	[14], Fig. 2(b)	2.07	f	twin-free, 82–86 K	VSM
YBa ₂ Cu ₃ O _{7-δ}	[13], Fig. 4	1.33	j	87–88 K	VSM, TR
YBa ₂ Cu ₃ O _{7-δ}	[15], Fig. 2(b)	1.03	j	No. 1, $d = 1.1$ mm, 50 K	VSM
YBa ₂ Cu ₃ O _{7-δ}	[15], Fig. 2(b)	1.54	j	No. 2, $d = 0.9$ mm, 30–50 K	VSM
YBa ₂ Cu ₃ O _{6.92}	[16], Fig. 3	2.17	j	C1, MT, twinned, 60 K	VSM
YBa ₂ Cu ₃ O _{6.96}	[17], Fig. 2(a)	1.85, 3.35	j	WU4, 60 K, 72–88 K	VSM
YBa ₂ Cu ₃ O _{7-δ}	[20], Fig. 3	2.23	j	MT, 50–75 K	SE
YBa ₂ Cu ₃ O _{7-δ}	[20], Fig. 14	2.75	f	60–87 K	SE
YBa ₂ Cu ₃ O _{7-δ}	[21], Fig. 3	1.79	f	C1, $d = 1.2$ mm, 70–83 K	SQUID
(Y _{0.8} Pr _{0.2})Ba ₂ Cu ₃ O _{7-δ}	[12], Fig. 1b	0.86	j	20 K	SQUID

“ n ” denotes the fitting parameter from Eqs. (1) and (7), “D” describes the scaling mode (j = critical current, f = pinning force density), “Method” means the experimental technique, “TR” = transport measurements, “SE” = sample extraction method, “MT” = melt-textured. “Note” denotes sample number according to the reference, temperature range and other details.

the fit is documented in Fig. 1. In the figures either the temperature range, or a single temperature is given indicating the temperature range of a good experimental data scaling. Data out of the indicated temperature range were either missing or the curves did not scale well. A single temperature indicates a single normalised, non-scaling curve.

Fig. 1(a) shows the fit by Eq. (1) of the $j_{sc}(b)$ dependence for a Y-123 single crystal in the temperature range 72–88 K where a good scaling was observed [17] (open squares). In this figure also the data for 60 K are indicated (departing from the

scaled ones) and their fit by the same function as before, only with a different n value. Fig. 1(c) documents on a Y-123 single crystal the difference of the fits by Eq. (7) (dotted curve) and by the function $3b^2(1 - 2/3b)$ (solid curve) used in the original paper [14]. A similar comparison is seen in Fig. 1(e). As in this case Eq. (7) fitted the data on a Y-123 single crystal [21] well only above the maximum (dashed curve), we fitted the low-field part separately (dotted curve). Again, the same function with only a different n value fits the curve perfectly. The hysteresis loops measured on Tm-123 single

Table 2
Comparison of the scaling properties of (RE)-123 and (KBa)BiO₃ (isotropic) samples

Material	Reference	n	D	Note	Method
YbBa ₂ Cu ₃ O _{7-δ}	[2], Fig. 1(b)	0.98	j	Göttl, 50 K	SQUID
DyBa ₂ Cu ₃ O _{7-δ}	[8], Fig. 3(a)	0.565	j	No. 4, twin-free s.c., 10–60 K	VSM
DyBa ₂ Cu ₃ O _{7-δ}	[22], Fig. 1(a)	0.5	j	AD, twin-free s.c., 10–40 K	TM
NdBa ₂ Cu ₃ O _{7-δ}	[23], Fig. 2	3.13	j	twinned, 5–86 K	SQUID
TmBa ₂ Cu ₃ O _{6.8}	[24], Fig. 1(b)	1.45	j	twinned, 20–82 K	VSM
TmBa ₂ Cu ₃ O _{6.45}	[17], Fig. 2(b)	0.85, 1.98	j	Z5, 5 K, 50 K	VSM
TmBa ₂ Cu ₃ O _{6.8}	[6]	1.0	m	N/A	VSM, DR
K _{0.4} Ba _{0.6} BiO ₃	[25], Fig. 1	1.5	j	No. 1, 2–20 K	PF, SQUID, VSM
K _{0.4} Ba _{0.6} BiO ₃	[26], Fig. 7	1.64	f	No. 1, 8 K	PF, SQUID, VSM

Columns as in Table 1. “m” = model analysis, “TM” = torque magnetometry, “DR” = dynamic relaxation.

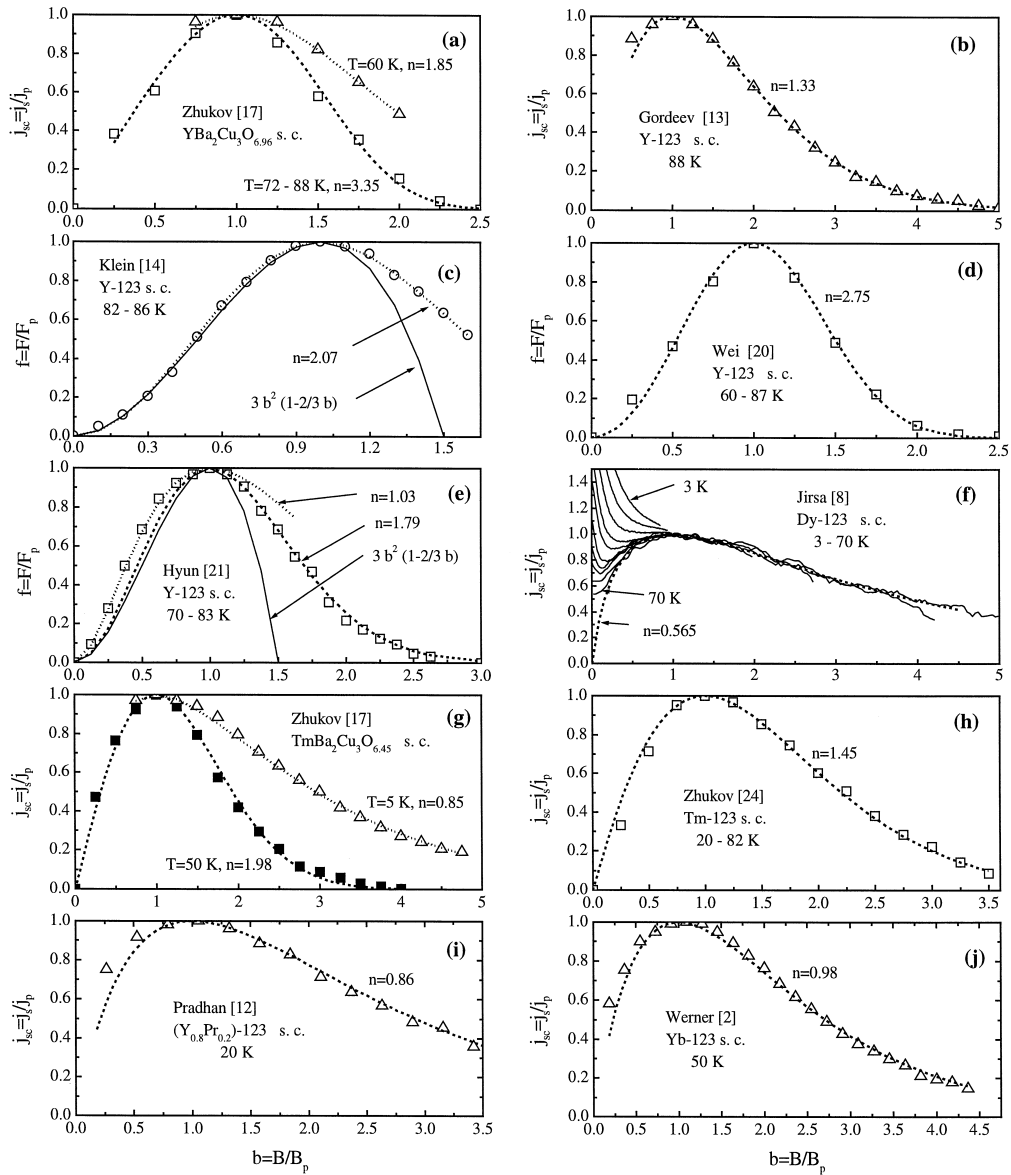


Fig. 1. Fit of the experimental $j_{sc}(b)$ and $f(b_f)$ dependencies reconstructed from data found in literature. (a) Fit of the normalised $j_s(B)$ curves scaling between 72 and 88 K and of the curve out of the scaling range (60 K) taken from Ref. [17], Fig. 2(a), (b) Ref. [13], Fig. 4, (c) Ref. [14], Fig. 2(b), (d) Ref. [20], Fig. 14, (e) Ref. [21], Fig. 3, (f) Ref. [8], Fig. 3(a), (g) Ref. [17], Fig. 2(b), (h) Ref. [24], Fig. 1(b), (i) Ref. [12], Fig. 1(b), (j) Ref. [2], Fig. 1(b). The dotted and dashed lines correspond to fits by either Eq. (1) or Eq. (7) with $m = 1$ and the n value as indicated in the figure. The full curves in (c) and (e) show the original fits used in the given references.

crystals [17] did not scale and could be fitted in the temperature range 5 to 50 K by Eq. (7) only with a temperature dependent n . Fig. 1(g) shows the nor-

malised curves $j_{sc}(b)$ for Tm-123 single crystals for the limiting 5 and 50 K. Again, Eq. (1) fits both curves quite well though with different n .

4. Discussion

Summarising the results, we can say that all the analyzed $j_s(B)$ dependencies exhibiting the fishtail shape, both in the $j_{sc}(b)$ and $f(b_f)$ representation, could be well fitted by expressions Eqs. (1) and (7), respectively, with $m = 1$ and the only free parameter n . Values of n varied between 0.5 and 3.95 but most values were found between 1 and 2, just around the value $n = 3/2$, corresponding to the theoretical value for the pinning of small bundles [43–47].

The rare cases with $n \ll 1$, namely the Dy-123 single crystals [8,22], Fig. 1(f), and the Y-123 single crystal No. 6 in Ref. [9], correspond to an extremely flat $j_s(B)$ dependence. The reason for this behaviour remains unclear. Zhukov et al. [17,3] also observed flat magnetisation curves but neither of their explanations, due to twin boundaries [3], and due to the particular (rather high) oxygen deficiency leading to a shape with two peaks or a plateau at high fields, is applicable to our case. The Dy-123 samples are twin-free and exhibit considerably higher critical current densities than those observed by Zhukov et al., without any evidence of a double-high-field-peak structure.

Also the large n values were mostly connected with an atypical $j_s(B)$ dependence:

- Only the high-field edge of a pronounced plateau at intermediate fields exhibited by the pure Y-123 single crystal 2515B of Delin et al. [5] was analyzed. A similar character had also the data of Ni-doped Y-123 single crystals [5].
- The fishtail peak on the MHL of the Nd-123 single crystal [23] was disturbed by another, field-independent, maximum lying just below and overlapping with the fishtail peak.
- The melt-textured samples of Wei et al. [20] exhibited a rather steep field dependence both of the critical currents and the associated pinning force density, Fig. 1(d). In this case, however, an incomplete alignment and porosity of the sample could play a significant role.

A different atypical shape of the MHL with a fishtail character was observed by Zhukov et al. [3] on a detwinned Y-123 single crystal. In this case, the $j_s(B)$ curve could be well fitted by Eq. (1) only separately below and above the maximum. The cor-

responding n values were significantly different ($n = 1.05$ and 1.8 , respectively).

Excluding these extreme cases, most of the analyzed experimental data, measured on a wide variety of high- T_c samples and detected by different experimental techniques, show very similar behaviour. It can be well described by Eq. (1) with $m = 1$ and n close to $3/2$, the value corresponding to the pinning regime of small vortex bundles [43–47]. In spite of the fact that this regime should apply only for fields $B > B_{sb} \approx 2B_{jp}$, most experimental curves can be fitted by the same functional dependence even at fields well below B_{jp} . It implies that such a type of a functional dependence has much more general validity than given by the theory of collective pinning.

While the origin of the fishtail maximum in RE-123 compounds from the crystallographic point of view seems to be clear now [17–19], an open question remains of the reason for a high-field pinning ability of the oxygen deficient zones or other impurities or, in other words, of the positive slope of $j_s(B)$ at low fields.

The phenomenological model of the thermally activated creep [6,7] can be applied also to the fields well below the fishtail maximum as there are no intrinsic limitations as in the theory of collective pinning. This model gives a rather surprising but reasonable explanation for the drop of j_s at fields below the fishtail maximum based on an interplay of different field dependencies of two quantities taking part in the relaxation process, namely the characteristic critical current density j_0 and the characteristic activation energy U_0 . Perkins et al. showed [6,7] that scaling properties imply the power-law dependencies of both $j_0(B)$ and $U_0(B)$. For Tm-123 single crystals these functions were found to be linear and inversely proportional, respectively. While the linear dependence of $j_0(B)$ seems to be quite general, the power of B in the $U_0(B)$ dependence is evidently controlled by the actual pinning structure present in the sample. In terms of this model, the fishtail minimum is a result of the interplay between the high-field pinning regime that loses its efficiency at low fields and the central peak that contributes to the total critical current only at low fields, typically below the field of penetration but rapidly drops with increasing field [8].

The narrow range of n values around $n = 3/2$ indicates that the pinning structure influences the MHL shape at high fields only indirectly, the main role being played by the collective pinning phenomena. The pinning regime at fields well above the fishtail maximum is probably determined mostly by the collective pinning of small bundles.

Irrespective of the sample quality, the temperature interval where $j_s(B)$ curves scale well according to Eq. (1) and/or Eq. (7) varies from sample to sample being sometimes only a few K wide while for other samples a good scaling is observed within nearly all the range of superconductivity [17]. It indicates that quality of the vortex lattice is strongly sample sensitive and probably different pinning regimes coexist under the same external conditions. The scaling effect can be then understood as a manifestation of the only one, well defined, pinning regime. This is clearly demonstrated in Ref. [8] on Dy-123 single crystals (see also Fig. 1(f)) where two contributions to the irreversible magnetisation were separated. The high-field one, scaled according to Eq. (1), goes to zero at zero field while the low-field one, responsible for the central peak on MHL, decays nearly exponentially with increasing field. This part has a steep temperature dependence resulting in a rapid reduction of the ratio of the central and fishtail peak with increasing temperature. We believe that this low-field pinning mechanism is responsible for a quite systematic positive deviation of the low-field data in Fig. 1(a),(b),(d),(f),(g),(i),(j), i.e. for all $j_{sc}(b)$ dependencies except the data on Tm-123 in Fig. 1(h). On the low-field part of the $f(b_f)$ dependencies the effect of the central peak is somewhat suppressed but has also to be taken into account.

Finally, it is worth noting that Eqs. (1) and (7) fit the experimental MHL data surprisingly well even in the case when the curves do not scale well (see Fig. 1(a),(g)). It implies that this type of functional dependencies might have a quite general validity.

5. Summary

In summary, we have presented simple analytical formulas for universal curves of scaled critical current and pinning force densities and shown their close relationship to the collective pinning regime of

small bundles. The expressions were tested on experimental data obtained on a large variety of (RE)-123 single crystals and some other high- T_c samples presented in literature. The data were measured by means of practically all commonly used experimental techniques. It was shown that the normalised experimental curves could be well fitted by the analytical formulas Eqs. (1) and (7) with $m = 1$ and the n value varied from 0.5 to 3.9. Most n values, however, dropped between 1 and 2, around $3/2$ corresponding to the pinning regime of small vortex bundles.

The simple fit presented here points to the importance of the pinning regime of small bundles. However, this pinning regime has its field domain at fields twice as high as the fishtail maximum position and higher [45]. The fact that the fit was found to be good also at fields well below the small bundle limit B_{sb} implies that the expressions Eqs. (1) and (7) for the fishtail-like field dependence of the critical currents and pinning force density in (RE)-123 materials are quite general and do not need necessarily originate only from the small bundle pinning regime.

Acknowledgements

This work was partly supported by GA ASCR (Grant No. A 1010512). The authors are grateful to Dr. M.R. Koblishka for the challenging discussion and valuable comments to this work.

References

- [1] M. Däumling, J.M. Seuntjens, D.C. Larbalestier, Nature 346 (1990) 332.
- [2] M. Werner, F.M. Sauerzopf, H.W. Weber, B.D. Veal, F. Licci, K. Winzer, M.R. Koblishka, Physica C 2833 (1994) 235–240.
- [3] A.A. Zhukov, H. Küpfer, H. Claus, H. Wühl, M. Kläser, G. Müller-Vogt, Phys. Rev. B 52 (1995) R9871.
- [4] J.L. Vargas, D.C. Larbalestier, Appl. Phys. Lett. 60 (1992) 1741.
- [5] K.A. Delin, T.P. Orlando, E.J. McNiff Jr., S. Foner, R.B. van Dover, L.F. Schneemeyer, J.V. Waszczak, Phys. Rev. B 46 (1992) 11092.
- [6] G.K. Perkins, L.F. Cohen, A.A. Zhukov, A.D. Caplin, Phys. Rev. B 51 (1995) 8513.
- [7] G.K. Perkins, D. Caplin, Phys. Rev. B 54 (1996) 12551.

- [8] M. Jirsa, L. Půst, D. Dlouhý, M.R. Koblishka, *Phys. Rev. B* 55 (1997) 3276.
- [9] L. Civale, M.W. McElfresh, A.D. Marwick, F. Holtzberg, C. Feil, J.R. Thompson, D.K. Christen, *Phys. Rev. B* 43 (1991) 13732.
- [10] M.S. Osafsky, J.L. Cohn, E.F. Skelton, M.M. Miller, R.J. Soulen Jr., S.A. Wolf, *Phys. Rev. B* 45 (1992) 4916.
- [11] A.A. Zhukov, H. Küpfer, S.N. Gordeev, W. Jahn, T. Wolf, V.I. Voronkova, A. Erb, G. Müller-Vogt, H. Wühl, H.J. Bornemann, K. Salama, D. Lee, in: H.W. Weber (Ed.), *Critical Currents in Superconductors*, World Scientific, Singapore, 1994, p. 229.
- [12] A.K. Pradhan, S.B. Roy, P. Chaddah, C. Chen, B.M. Wanklyn, *Physica C* 225 (1994) 269.
- [13] S.N. Gordeev, W. Jahn, A.A. Zhukov, H. Küpfer, W. Jahn, *Phys. Rev. B* 49 (1994) 15420.
- [14] L. Klein, E.R. Yacoby, Y. Yeshurum, A. Erb, G. Müller-Vogt, V. Breit, H. Wühl, *Phys. Rev. B* 49 (1994) 4403.
- [15] M. Oussena, P.A.J. de Groot, A. Marshall, J.S. Abel, *Phys. Rev. B* 49 (1994) 1484.
- [16] M. Oussena, P.A.J. de Groot, S.J. Porter, R. Gagnon, L. Taillefer, *Phys. Rev. B* 51 (1995) 1389.
- [17] A.A. Zhukov, H. Küpfer, G. Perkins, L.F. Cohen, A.D. Caplin, S.A. Klestov, H. Claus, V.I. Voronkova, T. Wolf, H. Wühl, *Phys. Rev. B* 51 (1995) 12704.
- [18] A. Erb, J.-Y. Genoud, F. Marti, M. Däumling, E. Walker, R. Flükiger, *J. Low Temp. Phys.* 105 (1996) 1023.
- [19] M. Däumling, A. Erb, E. Walker, J.-Y. Genoud, R. Flükiger, *Physica C* 257 (1996) 371.
- [20] C.D. Wei, Z.X. Liu, H.T. Ren, L. Xiao, *Physica C* 260 (1996) 130.
- [21] O.B. Hyun, M. Yoshida, T. Kitamura, I. Hirabayashi, *Physica C* 258 (1996) 365.
- [22] M. Jirsa, A.J.J. van Dalen, M.R. Koblishka, G. Ravi Kumar, R. Griessen, in: H.W. Weber (Ed.), *Critical Currents in Superconductors*, World Scientific, Singapore, 1994, p. 221.
- [23] M.R. Koblishka, A.J.J. van Dalen, T. Higuchi, K. Sawada, S.I. Yoo, M. Murakami, *Phys. Rev. B* 54 (1996) R6893.
- [24] A.A. Zhukov, H. Küpfer, S.A. Klestov, V.I. Voronkova, V.K. Yanovsky, *J. Alloys Compounds* 195 (1993) 479.
- [25] W. Harnleit, T. Klein, L. Baril, C. Escribe-Filippini, *Europhys. Lett.* 36 (1996) 141.
- [26] W. Harnleit, T. Klein, C. Escribe-Filippini, H. Rakoto, J.M. Broto, A. Sulpice, R. Buder, J. Marcus, W. Schmidbauer, *Physica C* 267 (1996) 270.
- [27] K. Kadowaki, T. Mochiku, *Physica C* 195 (1992) 127.
- [28] M. Xu, D.K. Finnemore, G.W. Crabtree, V.M. Vinokur, B. Dabrowski, D.G. Hinks, K. Zhang, *Phys. Rev. B* 48 (1993) 10630.
- [29] Ming Xu, K. Zhang, B. Dabrowski, in: A.V. Narlikar (Ed.), *Studies of High Temperature Superconductors*, vol. 14, Nova Science, New York, 1994.
- [30] K. Kishio, J. Shimoyama, Y. Kotaka, K. Yamafuji, in: H.W. Weber (Ed.), *Critical Currents in Superconductors*, World Scientific, Singapore, 1994, p. 339.
- [31] T. Tamegai, S. Ooi, T. Shibauchi, Y. Matsushita, M. Hasegawa, H. Takei, M. Ichihara, K. Suzuki, *Physica C* 2817 (1994) 235–240.
- [32] S. Ooi, T. Tamegai, T. Shibauchi, *Physica C* 259 (1996) 280.
- [33] S. Ooi, T. Tamegai, T. Shibauchi, *J. Low Temp. Phys.* 105 (1996) 1011.
- [34] X.Y. Cai, A. Gurevich, D.C. Larbalestier, R.J. Kelley, M. Onellion, H. Berger, G. Margaritondo, *Phys. Rev. B* 50 (1994) 16774.
- [35] Ch. Goupil, A. Ruyter, J. Provost, T. Aouaroun, Ch. Simon, *J. Phys. III (France)* 5 (1995) 1481.
- [36] Y. Yamaguchi, N. Aoki, F. Iga, Y. Nishihara, *Physica C* 246 (1995) 216.
- [37] D.H. Ha, K.W. Lee, K. Oka, Y. Yamaguchi, F. Iga, Y. Nishihara, *Physica C* 260 (1996) 242.
- [38] B. Khaykovich, E. Zeldov, D. Majer, T.W. Li, P.H. Kes, M. Konczykowski, *Phys. Rev. Lett.* 76 (1996) 2555.
- [39] M. Kiuchi, E.S. Otabe, T. Matsushita, T. Kato, T. Hikata, K. Sato, *Physica C* 260 (1996) 177.
- [40] A. Wisniewski, R. Szymczak, M. Baran, R. Puzniak, J. Karpinski, R. Molinski, H. Schwer, K. Conder, I. Meijer, *Czech. J. Phys.* 46 (Suppl. S3) (1996) 1950.
- [41] L. Půst, M. Jirsa, L. Papadimitriou, O. Valassiadis, C.B. Lioutas, *Acta Phys. Slovaca* 46 (1996) 183.
- [42] H.G. Schnack, R. Griessen, J.G. Lensink, Wen Hai-Hu, *Phys. Rev. B* 48 (1993) 13178.
- [43] G. Blatter, M.V. Geshkenbein, A.I. Larkin, V.M. Vinokur, *Rev. Mod. Phys.* 66 (1994) 1125.
- [44] M.V. Feigel'man, V.B. Geshkenbein, A.I. Larkin, V.M. Vinokur, *Phys. Rev. Lett.* 63 (1989) 2303.
- [45] A.E. Koshelev, V.M. Vinokur, *Physica C* 173 (1991) 465.
- [46] V.M. Vinokur, P.H. Kes, A.E. Koshelev, *Physica C* 168 (1990) 29.
- [47] M.V. Feigel'man, V.M. Vinokur, *Phys. Rev. B* 41 (1990) 8986.